UvA-DARE (Digital Academic Repository)

Elevated CO2 and Phosphate Limitation Favor Micromonas pusilla through Stimulated Growth and Reduced Viral Impact

Maat, D.S.; Crawfurd, K.J.; Timmermans, K.R.; Brussaard, C.P.D.

[Link to publication](#)

![AEM Journals.ASM.org logo]

Elevated CO_2 and Phosphate Limitation Favor *Micromonas pusilla* through Stimulated Growth and Reduced Viral Impact

Douwe S. Maat,[a] Katherine J. Crawfurd,[a] Klaas R. Timmermans,[a] Corina P. D. Brussaard[a,b]

Department of Biological Oceanography, NIOZ-Royal Netherland Institute for Sea Research, Den Burg, The Netherlands[a]; Aquatic Microbiology, Institute for Biodiversity and Ecosystem Dynamics, University of Amsterdam, Amsterdam, The Netherlands[b]

Growth and viral infection of the marine picoeukaryote *Micromonas pusilla* was studied under a future-ocean scenario of elevated partial CO_2 (pCO_2; 750 μatm versus the present-day 370 μatm) and simultaneous limitation of phosphorus (P). Independent of the pCO_2 level, the ratios of *M. pusilla* cellular carbon (C) to nitrogen (N), C:P and N:P, increased with increasing P stress. Furthermore, in the P-limited chemostats at growth rates of 0.32 and 0.97 of the maximum growth rate (μ_{max}), the supply of elevated pCO_2 led to an additional rise in cellular C:N and C:P ratios, as well as a 1.4-fold increase in *M. pusilla* abundance. Viral lysis was not affected by pCO_2, but P limitation led to a 150% prolongation of the latent period (6 to 12 h) and an 80% reduction in viral burst sizes (63 viruses per cell) compared to P-replete conditions (4 to 8 h latent period and burst size of 320). Growth at 0.32 μ_{max} further prolonged the latent period by another 150% (12 to 18 h). Thus, enhanced P stress due to climate change-induced strengthened vertical stratification can be expected to lead to reduced and delayed virus production in picoeukaryotes. This effect is tempered, but likely not counteracted, by the increase in cell abundance under elevated pCO_2. Although the influence of potential P-limitation-relieving factors, such as the uptake of organic P and P utilization during infection, is unclear, our current results suggest that when P limitation prevails in future oceans, picoeukaryotes and grazing will be favored over larger-sized phytoplankton and viral lysis, with increased matter and nutrient flow to higher trophic levels.

Anthropogenic CO_2 emissions are expected to lead to a doubling of the ~390 μatm present-day partial CO_2 (pCO_2) pressure by the year 2100 (1). A large part of this CO_2 will be taken up by the world's oceans, where it will lead to a decrease in pH and a shift in carbon speciation (2). These changes are expected to have consequent effects on marine photoautotrophs, which depend on dissolved inorganic carbon (DIC) for their photosynthesis. Thus far, studies on the effects of elevated pCO_2 on phytoplankton have shown divergent outcomes, ranging from no effects to changes in growth rate, primary production, and elemental stoichiometry (3). The effects of elevated pCO_2 on diatoms, coccolithophores, and cyanobacteria have been studied in the laboratory in greater detail, but to our knowledge there is only one other study in which the effects of elevated pCO_2 on picoeukaryotes was studied in the laboratory under well-controlled conditions (4). It has been hypothesized that diffusion of CO_2 typically is not expected to limit photosynthesis in the very-small-sized phytoplankton (5). However, carbon-concentrating mechanisms were identified in the genome of the picophytoplankter *Micromonas pusilla* (6). An extensive experiment in the Arctic by Brussaard et al. (7), comprising 9 mesocosms with a pCO_2 increasing from 180 to 1,100 μatm, showed a significant increase in the abundance of picoeukaryotic photoautotrophs with CO_2 concentration. An increase of picoeukaryotic *Micromonas*-like cells was also observed in a nutrient-replete mesocosm study under elevated pCO_2 (8). More recently, during a similar mesocosm experiment in the same Norwegian fjord, an increase in form 1B *rbcL* sequences similar to that of *Micromonas* spp. was observed (9).

Micromonas pusilla is an important member of the picophytoplankton community worldwide and is found from coastal to oceanic ecosystems and from the poles to the equator (10, 11). This prasinophyte is readily infected by viruses, and viral lysis is an important loss factor for this species (12, 13). The importance of viruses in structuring marine microbial communities and as drivers of biogeochemical cycles has well been recognized (14–17); however, only a limited number of studies have actually focused on the effects of growth-limiting factors on algal host-virus interactions (18–22). An important macronutrient often limiting phytoplankton growth in many ecosystems worldwide is phosphorus (P) (23). In addition, P limitation is suggested to be particularly important for viral replication due to the relatively low C:P ratios of viruses compared to those of their hosts (18). P depletion has been reported to induce lysogeny in *Synechococcus* sp. strain WH7803 and reduce virus production for viruses infecting *Emiliania huxleyi*, *Phaeocystis pouchetii*, and *Chlorella* sp. strain NC64A (18–20, 22). To our knowledge, no data are available for picoeukaryotes that are theoretically better adapted to low nutrient availability than larger phytoplankton species (24). Global climate change-induced warming of the ocean surface will strengthen vertical stratification in large parts of the world's oceans and enhance nutrient limitation for phytoplankton growth (25, 26). Under such conditions, viruses would have an even more critical function as drivers of microbial activity and nutrient recycling.

In the present study, we investigated the simultaneous effects of elevated pCO_2 and P limitation on *M. pusilla* growth characteristics and its interaction with a lytic *M. pusilla* virus (MpV). Axenic cultures of *M. pusilla* were subjected to present-day and future

pCO$_2$ levels by constant aeration of synthetic air. P-limiting growth (0.32 and 0.97 of the maximum growth rate [μ_{max}]) was derived by chemostat culturing, in which the continuous inflow rate of P-limited medium determined the growth rate of the phytoplankton cells and forced the cells into a steady physiological condition. At steady state, cultures were sampled for growth characteristics in the period preceding the viral infection experiments. P-replete cultures at 1.0 μ_{max} were used as a reference.

MATERIALS AND METHODS

Culturing and experimental setup. Axenic cultures of the prasinophyte *Micromonas pusilla* (Mp-Lac38; Marine Research Center culture collection, Göteborg University) and viral lysate of the double-stranded DNA (dsDNA) *M. pusilla* virus MpV-08T (NIOZ Culture Collection, The Netherlands) were used. Axenic lysate of MpV-08T was prepared by three infection cycles using algal host grown at the specific culture conditions (i.e., P limited or P replete). The infectivity of MpV, as tested by MPN endpoint dilution (27), was 100%; thus, it was not affected by P or pCO$_2$ treatment. Axenity of the algal cultures and viral lysate were checked by epifluorescence microscopy using the nucleic acid stain 4′,6-diamidino-2-phenylindole (DAPI; Life Technologies Ltd., Paisley, United Kingdom). At all times during the experiment the cultures were axenic.

M. pusilla was grown in 5-liter borosilicate chemostat culture vessels with P as the algal growth-limiting nutrient and with water jackets connected to a water bath (Lauda Ecoline StarEdition RE104; Lauda, Königshofen, Germany) to keep the temperature at 15°C. The cultures were stirred by a glass clapper above a magnetic stirrer, moving at 15 rpm. Irradiance at 100 μmol quanta m^{-2} s^{-1} was supplied by 18W/965 Osram daylight-spectrum fluorescent tubes (Munich, Germany) in a light:dark cycle of 16:8 h. The cultures were grown in filtered (0.1-μm polyethersulfone membrane filter; Sartopore Midicap; Sartorius A.G., Goettingen, Germany) f/2 medium (28) that was modified to contain 0.25 μM Na$_2$HPO$_4$, 40 μM NaNO$_3$, and 0.01 μM Na$_2$SeO$_3$ (29). Algal growth rates were set by the dilution rate (continuous inflow of medium and similar rate of outflow of culture), i.e., 0.97 μ_{max} and 0.32 μ_{max}, where μ_{max} = 0.72 day^{-1}. Duplicate cultures were maintained for each treatment. The duplicate P-replete cultures were grown semicontinuously at 1.0 μ_{max} (keeping the algal abundance around 5.5 × 10^6 ml^{-1} by daily dilution) in similar 5-liter culture vessels and culture conditions, with the medium modified to contain 36 μM Na$_2$HPO$_4$ and 882 μM NaNO$_3$.

Before being added to the algal cultures, all media were equilibrated to the appropriate pCO$_2$ by aeration with synthetic air with either 370 or 750 μatm CO$_2$ (Messer B.V. Moerdijk, Netherlands). Additionally, the algal cultures received similar aeration with synthetic air at approximately 2.5 liters h^{-1} using glass bubble stones. Aeration was chosen as the closest representative of DIC supply in simulating natural conditions compared to other methods (30, 31). The pCO$_2$ from the vessel air outlets was continuously analyzed by infrared CO$_2$ probes (Vaisala Carbocap carbon dioxide probe GMP343; Vantaa, Finland) to allow adaptation of the aeration rate if necessary. During the viral infection experiments, aeration continued at identical rates.

The cultures were considered to be at steady state after at least 5 volume changes with constant algal abundances for more than 28 days. Sampling at steady state was performed approximately 3 h into the light period. Cultures were sampled for dissolved inorganic carbon (DIC), total alkalinity (A$_T$), dissolved inorganic phosphate (DIP), algal and viral abundance, flow-cytometric characteristics, photosynthetic capacity, alkaline phosphatase activity (APA), net primary production (NPP), pigment composition, and particulate organic carbon (POC) and nitrogen (PON).

For the viral infection experiments, the 5-liter cultures at steady state were infected 3 h into the light period with MpV-08T at a virus-to-algal-host ratio of 10 to allow one-step infection. At the moment of infection the medium pumps were stopped, while aeration continued to maintain the specific pCO$_2$ supply throughout the viral infection experiment. The non-infected control cultures received filtered (0.2-μm-pore-size cellulose ac-

TABLE 1 Steady-state averages of culture pCO$_2$, DIC, A$_T$, and pH after cellular uptake of inorganic carbon[a]

pCO$_2$ input (μatm) and P level	pCO$_2$ (μatm)	DIC (μmol kg^{-1})	A$_T$ (μmol kg^{-1})	pH
370				
0.32 μ_{max}	291 ± 37	2,103 ± 10	2,450 ± 24	8.10 ± 0.01
0.97 μ_{max}	256 ± 15	2,079 ± 5	2,451 ± 36	8.17 ± 0.04
P replete	207 ± 16	2,175 ± 21	2,695 ± 19	8.23 ± 0.03
750				
0.32 μ_{max}	510 ± 36	2,235 ± 3	2,471 ± 13	7.93 ± 0.02
0.97 μ_{max}	459 ± 25	2,210 ± 10	2,465 ± 18	7.92 ± 0.01
P replete	420 ± 35	2,315 ± 25	2,655 ± 30	8.02 ± 0.03

[a] Cellular uptake of inorganic carbon was supplied by aeration, and the input of medium was equilibrated to 370 and 750 μatm CO$_2$. Results are averages ± SE.

etate; Sartorius A.G., Goettingen, Germany), autoclaved seawater at the same volume. Cultures were sampled for DIC (days 1 and 3), DIP, algal and viral abundances, flow-cytometric characteristics, and NPP (once a day). The viral infection experiments using P-limited chemostats at 370 and 750 μatm were repeated (9 months between experiments) for viral and algal abundances but unfortunately failed for the 0.97-μ_{max} growth condition due to technical reasons. The 0.32-μ_{max} culture replicates were very similar, with low standard deviations and identical latent period and burst size (62 ± 2).

Algal and viral abundances. Samples for algal and viral counts were analyzed by flow cytometry (32, 33). In short, 1-ml samples of *M. pusilla* were counted fresh using a BD Accuri C6 cytometer (BD Biosciences, San Jose, CA), with the trigger on chlorophyll red autofluorescence. Virus samples were fixed with 25% gluteraldehyde (electron microscopy [EM] grade; 0.5% final concentration; Sigma-Aldrich, St. Louis, MO, USA), incubated for 30 min at 4°C, flash frozen in liquid nitrogen, and stored at −80°C until analysis. Upon thawing, the samples were diluted 100- to 1,000-fold in filtered (0.2-μm pore size; FP 30/0.2 CA-S; Whatman, Dasser, Germany) Tris-EDTA buffer (pH 8) and stained with SYBR green I to a final concentration of 0.5 × 10^{-4} of the commercial stock (Life Technologies Ltd., Paisley, United Kingdom) for 10 min at 80°C. Sample analysis was carried out on a benchtop BD FACSCalibur (BD Biosciences, San Jose, CA, USA) with a 488-nm argon laser with the trigger set on green fluorescence. Flow cytometry behavior was tested using BD Trucount tubes (BD Biosciences, San Jose, CA, USA), and flow rates were determined by weight measurements according to reference 32. All flow cytometry data were analyzed using CYTOWIN 4.31 (34). The viral burst sizes were subsequently calculated by dividing the number of newly produced viruses by the number of host cells that lysed.

Chemical analyses. To determine the inorganic carbon concentrations and speciations in the cultures, 250-ml samples were fixed with 50 μl saturated HgCl$_2$ solution and stored in the dark at 15°C until analysis (35, 36). DIC and A$_T$ subsequently were determined by a Vindta 3C (versatile instrument for the determination of total inorganic carbon and titration alkalinity; Marianda, Germany). Certified reference material (CRM) was included in the measurements (36). Culture CO$_2$ concentrations were calculated from DIC and A$_T$ using the program CO$_2$sys (37), applying the equilibrium constants of Mehrbach (38) and Dickson and Millero (39) and accounting for salinity and inorganic phosphorus concentrations. Table 1 shows the resultant pCO$_2$, DIC, A$_T$, and pH in the cultures. The resultant pCO$_2$ in the culture vessels at steady state was constant but reduced compared to the input level (370 and 750 μatm) as a consequence of cellular uptake (40). However, increasing the aeration rate even more to compensate for the high uptake was not possible due to inhibiting effects on *M. pusilla* growth. pCO$_2$ ($P < 0.001$; Kruskall-Wallis), DIC, and pH ($P < 0.001$ for both parameters; 2-way analysis of variance [ANOVA]) showed a statistically significant difference between the present-day and

future treatments. Within each pCO_2 treatment, total DIC did not differ between the 0.32- and 0.97-μ_{max} P treatments ($P = 0.065$) but was slightly higher for the P-replete treatments ($P < 0.001$). This coincided with a higher alkalinity for this treatment ($P < 0.001$), which was a direct result of phosphate dissolution. Within the P-limited cultures, alkalinity was not significantly affected by growth rate or pCO_2 treatment. Moreover, during the viral infection experiment the pCO_2 in the culture medium was comparable to that in the steady state, on average 229 (± 17) and 435 (± 41) for present-day and future pCO_2, respectively.

DIP was determined colorimetrically as described by Hansen and Koroleff (41), with a lower limit of detection of 0.02 μM. Samples were filtered (0.2 μm; FP 30/0.2 CA-S; Whatman, Dasser, Germany) into clean screw-cap vials and stored at −20°C until analysis. DIP concentrations remaining in the culture medium at chemostat steady states were at the detection limit, i.e., as low as 0.023 (± 0.004) μM for all culture vessels and considered zero. As expected, the P-replete semicontinuous cultures still had high DIP concentrations of 30.5 $\pm$ 0.8 μM left at steady state. Dissolved inorganic nitrate concentrations at steady state were above 20 μM at all times for the infected and noninfected cultures under both P-replete and P-limiting conditions.

As a direct indicator of P limitation, APA was determined fluorometrically according to the method of Perry (42). To a glass cuvette with 2 ml of culture, 3-O-methylfluorescein phosphate (MFP; Sigma-Aldrich, St. Louis, MO, USA) was added to a final concentration of 595 μM. Emission at 510 nm was measured on a Hitachi F2500 fluorescence spectrophotometer (Tokyo, Japan) for 60 s at an excitation wavelength of 430 nm. The rate of MFP conversion was determined by comparing the values to a standard curve of 3-O-methylfluorescein (Sigma-Aldrich, St. Louis, MO, USA).

The particulate organic fractions of algal carbon (POC) and nitrogen (PON) were obtained on precombusted (4 h at 450°C) and preweighed 25-mm Whatman GF/F filters (Maidstone, Kent, United Kingdom) in triplicate. After storage at −20°C, the filters were weighed again, folded into tin (Sn) cups, and analyzed using a Thermo-Interscience Flash EA1112 series elemental analyzer (Waltham, MA, USA) (43). Particulate organic phosphorus (POP) was calculated as the difference between DIP from the medium and the culture.

Photosynthetic capacity of the *M. pusilla* cells was determined by PAM fluorometry (Water-PAM, Walz, Germany). After a 20-min dark incubation, the F0 and Fm chlorophyll *a* autofluorescence levels were determined and used to calculate the maximal photosynthetic efficiency as Fv/Fm, where Fv is the variable fluorescence and equals Fm minus F0 (44).

NPP was determined by the uptake of radiolabeled bicarbonate. Sixty ml of culture (2 duplicates, 1 dark control) was spiked with 10 μCi of $Na_2H^{14}CO_3$ (specific activity, 2 mCi mmol^{-1}; Amersham) and incubated for 3 h on an incubation wheel at 3 rpm under growth conditions similar to those used for the cultures but without separate pCO_2 treatment. Upon incubation, bottles were moved to the dark and directly filtered through a 47-mm Whatman GF/F filter (Maidstone, Kent, United Kingdom). The filters were then fumed above 30% HCl for 2 h to remove the remaining ^{14}C and stored in scintillation vials at −20°C. Twenty-four hours before analysis using a Tri-carb 2300 TR scintillation analyzer (Packard Instrument Company, LaGrange, IL, USA), 20 ml of scintillation cocktail (Filter-Count; PerkinElmer, Waltham, MA) was added to the filter. Total primary production was calculated as $\Delta C = (sa \times DIC \times 1.06)/(aa \times t)$, whereby ΔC is the carbon uptake rate (μmol C h^{-1}), sa is the sample activity (disintegrations per minute [DPM]), 1.06 is the isotope effect constant, aa is the added activity (DPM), and t is the incubation time (in hours) (45).

Pigment analysis on 50 ml GF/F-filtered (Maidstone, Kent, United Kingdom) frozen samples was performed by high-performance liquid chromatography (HPLC). This was carried out on a Dionex HPLC system equipped with a C_8 separation column (Luna 3μ$C_8$100A; 100 by 4.6 mm; Phenomenex, Torrance, CA, USA). Pigment extraction took place in 4 ml methanol using glass pearls in a CO_2-cooled Braun (Melsungen, Ger-

many) homogenizer. Pigments were detected at 437 nm with a Dionex photo diode array detector. The solvents were used according to Zapata et al. (46), and pigment standards were obtained from DHI (Hørsholm, Denmark). The individual pigment concentrations where then used to calculate the level of Chl *a*/cell, the Chl *a*/Chl *b* ratio, and the epoxidation state of the xanthophyll pigments [violaxanthin/(lutein + zeaxanthin)] as indicators of nutrient stress (47).

Statistical analysis. Using Sigmaplot 12.0 (Systat Software Inc., Chicago, IL, USA), two-way ANOVAs were carried out to determine the differences between the three phosphate and two pCO_2 treatment groups. When the assumptions for ANOVA could not be met in this way, nonparametric Kruskal-Wallis tests or one-way ANOVAs were carried out for each treatment group. Sample sizes ($n = 4$ to 6) for steady-state measurements are the results of duplicate vessels and the number of sampling days. A significance level of 0.05 was used, normality was verified by a Shapiro-Wilk test, and equal variances were verified by a Bartlett's test. Values in tables and the text are given as means $\pm$ standard errors (SE).

RESULTS

Steady-state algal physiology. Chemostat preculturing forced *M. pusilla* cells to be in a steady physiological growth phase under different degrees of P limitation (0.32 and 0.97 μ_{max}). Steady-state physiological and stoichiometric values are depicted in Table 2 (see Table S2 in the supplemental material for *P* values). *M. pusilla* abundance in the P-limited chemostats was 1.4-fold higher under future pCO_2 than under present-day pCO_2 values ($P < 0.001$; Kruskal-Wallis). No significant differences in cell abundance could be observed between the 0.32- and 0.97-μ_{max} cultures. Flow-cytometric cellular characteristics showed increasing forward scatter (FSC) with the degree of P limitation ($P < 0.001$); this was not significantly affected by pCO_2 treatment. Chlorophyll *a* red autofluorescence per cell (RFL) of the 0.97-μ_{max} P-limited cultures was lowest and was statistically different ($P < 0.001$) from the 0.32-μ_{max} and P-replete treatments. However, this was not reflected in the cellular Chl *a* content, where the values for 0.32- and 0.97-μ_{max} P-limited cultures did not differ significantly and were 2-fold lower than those for the P-replete ones ($P < 0.001$). The epoxidation state of the xanthophyll pigments of the 0.32-μ_{max} P-limited cells was about 2-fold lower than that of the 0.97-μ_{max} P-limited and P-replete cells ($P = 0.024$). The Fv/Fm ratio did show significant differences between all P treatments ($P < 0.001$), increasing from 0.32-μ_{max} P limited to P replete, and the same pattern was encountered for the Chl *a*/Chl *b* ratio ($P < 0.013$). None of these cellular photophysiological characteristics was significantly affected by pCO_2 treatment.

The alterations in (photo)physiology were reflected in the cellular NPP, with the 0.32- and 0.97-μ_{max} cultures showing a reduction of 70 and 44%, respectively, compared to the P-replete cultures. NPP was not significantly affected by pCO_2 ($P = 0.660$). APA per cell was, on average, 3.8-fold higher for the 0.32-μ_{max} than for the 0.97-μ_{max} P-limited chemostat cultures ($P < 0.001$) and was independent of pCO_2 ($P = 0.066$). The P-replete treatment showed no APA, in agreement with the high inorganic P concentration in these cultures.

The pCO_2 treatment significantly affected the cellular C:N and C:P ratios of the P-limited cultures, which were both higher under future pCO_2 ($P = 0.002$ and $P < 0.001$, respectively). No interaction effects between pCO_2 and P treatment on these ratios were found. The changes in C:N and C:P in the P-limited cultures likely are due to both an increase in cellular POC and a concomitant

TABLE 2 Steady-state algal characteristics under present-day and future pCO_2

	Value according to pCO_2 and P levels[b]					
	Present day (370 μatm)			Future (750 μatm)		
Algal characteristic[a]	0.32 μ_{max}	0.97 μ_{max}	P replete	0.32 μ_{max}	0.97 μ_{max}	P replete
M. pusilla abundance ($\times 10^5$ ml^{-1})	8.1 ± 0.0	7.8 ± 0.0	5.4 ± 0.1	11.1 ± 0.5	10.8 ± 0.2	5.5 ± 0.2
FSC (RU)	1.00 ± 0.0	0.56 ± 0.0	0.46 ± 0.0	0.99 ± 0.0	0.57 ± 0.0	0.45 ± 0.0
RFL (RU)	1.0 ± 0.0	0.8 ± 0.0	1.1 ± 0.0	1.0 ± 0.0	0.8 ± 0.0	1.1 ± 0.0
Fv/Fm (RU)	0.49 ± 0.0	0.61 ± 0.0	0.66 ± 0.0	0.49 ± 0.0	0.62 ± 0.0	0.66 ± 0.0
Chl *a* (fg cell^{-1})	9.76 ± 0.3	9.90 ± 0.3	21.5 ± 1.0	10.3 ± 0.2	10.4 ± 0.7	20.5 ± 2.3
Epoxidation state	1.8 ± 0.2	3.5 ± 0.1	3.2 ± 0.5	1.7 ± 0.4	3.0 ± 1.2	3.1 ± 0.0
Chl *a*/Chl *b*	0.95 ± 0.0	1.0 ± 0.0	1.2 ± 0.0	0.91 ± 0.0	1.1 ± 0.0	1.2 ± 0.0
NPP (pmol C cell^{-1} h^{-1})	1.43 ± 0.17	2.33 ± 0.17	3.77 ± 0.11	1.49 ± 0.24	2.34 ± 0.20	3.84 ± 0.21
APA (amol cell^{-1} s^{-1})	29.1 ± 0.14	8.38 ± 0.1	0.0	24.5 ± 0.29	5.61 ± 0.10	0.0
POC (fmol cell^{-1})	224 ± 1.2	146 ± 6.9	257 ± 6.9	241 ± 5.8	166 ± 8.1	246 ± 12.7
PON (fmol cell^{-1})	23.2 ± 3.3	14.8 ± 3.5	36.6 ± 2.2	16.5 ± 0.34	13.5 ± 0.34	33.9 ± 2.0
POP (fmol cell^{-1})	0.16 ± 0.0	0.18 ± 0.0	8.7 ± 0.84	0.12 ± 0.0	0.13 ± 0.0	8.0 ± 1.2
C:N	11 ± 0.5	9.3 ± 0.2	7.2 ± 0.3	15 ± 0.2	12 ± 0.3	7.5 ± 0.3
C:P	1,401 ± 8.1	823.8 ± 19	30.65 ± 1.3	2,227 ± 75	1,347 ± 51	33.01 ± 2.6
N:P	145 ± 9	83.2 ± 2	4.53 ± 0.1	151 ± 5	105 ± 3	4.50 ± 0.3

[a] Algal characteristics included *M. pusilla* cell abundance, forward scatter (FSC), chlorophyll *a* red autofluorescence (RFL), photosynthetic efficiency (Fv/Fm), chlorophyll *a* (Chl *a*) level, epoxidation state, Chl *a*/Chl *b* ratio, net primary production (NPP), alkaline phosphatase activity (APA), cellular carbon (POC), cellular nitrogen (PON), cellular phosphorus (POP), and cellular carbon:nitrogen (C:N), carbon:phosphorus (C:P), and nitrogen:phosphorus (N:P) ratios. Note that the algal abundances of the P-replete semicontinuous cultures should not be compared to the abundances of the P-limited chemostat cultures due to differences in culturing methods. RU, relative units.
[b] Results are averages ± SE.

decrease in cellular PON and POP under future pCO_2, but separately no statistically significant differences could be observed.

Considering the P treatments, cellular POC was significantly lower ($P = 0.003$) for the 0.97-μ_{max} P-limited treatment than the 0.32-μ_{max} and P-replete treatments. No significant pattern was observed for PON. Cellular PON and POP of both P-limited cultures were significantly different from the those of the P-replete ones ($P \leq 0.003$ and $P < 0.05$ for PON and POP, respectively). The C:N, C:P, and N:P ratios all were lower under P-limiting than under P-replete conditions ($P < 0.05$), where the C:P ratio was significantly affected by the growth rate (0.32 versus 0.97 μ_{max}).

Viral infection experiments. Viral infection resulted in full cell lysis for all cultures except the noninfected ones (Fig. 1). The onset of algal cell lysis upon viral infection of the P-limited cultures was delayed by approximately a day compared to the P-replete cultures (Fig. 1B). In the infected cultures, NPP was maintained far into the viral growth cycle (Fig. 2), although, compared to the noninfected controls, it was strongly reduced by viral infection under both pCO_2 treatments. The additional decrease in time of the noninfected controls was due to increasing P stress (Fig. 2). In concordance with the delayed algal host cell lysis, the release of progeny viruses appeared later and at a lower rate under P limitation than P-replete conditions (Fig. 3). The latent period was prolonged up to 3-fold under P limitation and was related to the extent of P depletion, i.e., 4 to 8, 6 to 12, and 12 to 18 h for P-replete, 0.97-μ_{max}, and 0.32-μ_{max} treatments, respectively. P limitation resulted in a 5-fold lower burst size compared to that of P-replete growth conditions for the algal host (63 ± 2 and 320 ± 7, respectively). Neither the degree of P limitation nor pCO_2 levels significantly affected the viral burst sizes in the P-limited cultures.
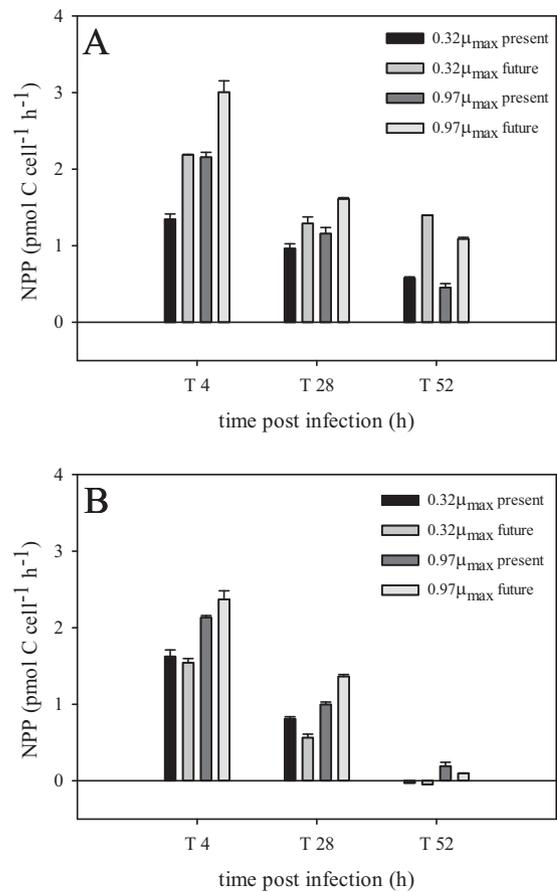
DISCUSSION

M. pusilla in the future ocean. Present and future ocean pCO_2 conditions (370 and 750 μatm CO_2, respectively) were simulated by the addition of equilibrated medium and synthetic air to the *M.*

pusilla cultures. Due to uptake of DIC by the algal cells, the resulting ambient pCO_2 in the cultures was lower than the set point. Increasing the aeration rate to compensate for the high DIC uptake by the algae was not possible due to the inhibiting effect on *M. pusilla* growth. A reduction of the cell abundances may have overcome the reduction of pCO_2 in the cultures compared to the set point but was not a desired setup for the viral infection experiments. Small variations in the culture pCO_2 within P treatments were the result of differential DIC uptake by the P-replete and 0.97-μ_{max} and 0.32-μ_{max} P-limited cultures and illustrate the differences in physiology between these cultures. Correcting for this by supplying differential pCO_2 would, however, affect the uptake and growth rates of the algal cultures, potentially influencing the virus-host interactions under study. In contrast to some studies maintaining the set point pCO_2 in the cultures (48, 49), our approach focused on supplying CO_2 as it is supplied under natural conditions. Similar reductions in pCO_2 have been observed in nature (40, 50). In order to keep the pCO_2 in the culture at the specific set points, however, higher DIC concentrations may have to be supplied than those experienced by the algae under natural present-day and future (simulating year 2100) conditions, with resultantly likely unrealistic effects on algal abundance and C:N:P ratios (this study). The most pronounced effect of elevated pCO_2, representing the predicted conditions of the year 2100 (1), was the 1.4-fold increase in *M. pusilla* abundance under P-limiting conditions. To our knowledge, there is only one other example of a similar response of a marine photoautotroph to such conditions, i.e., the haptophyte *Emiliania huxleyi* grown in P-controlled chemostats at a growth rate of 0.1 and 0.3 μ_{max} and at 900-μatm pCO_2 (48). In this study, the increase in cell abundance was accompanied by a 22% reduction in cell volume compared to the present-day pCO_2 values. However, in our study, the FSC of *M. pusilla*, which may be used as an indicator of cell size (51), did not show significant differences between the pCO_2 treatments. The in-
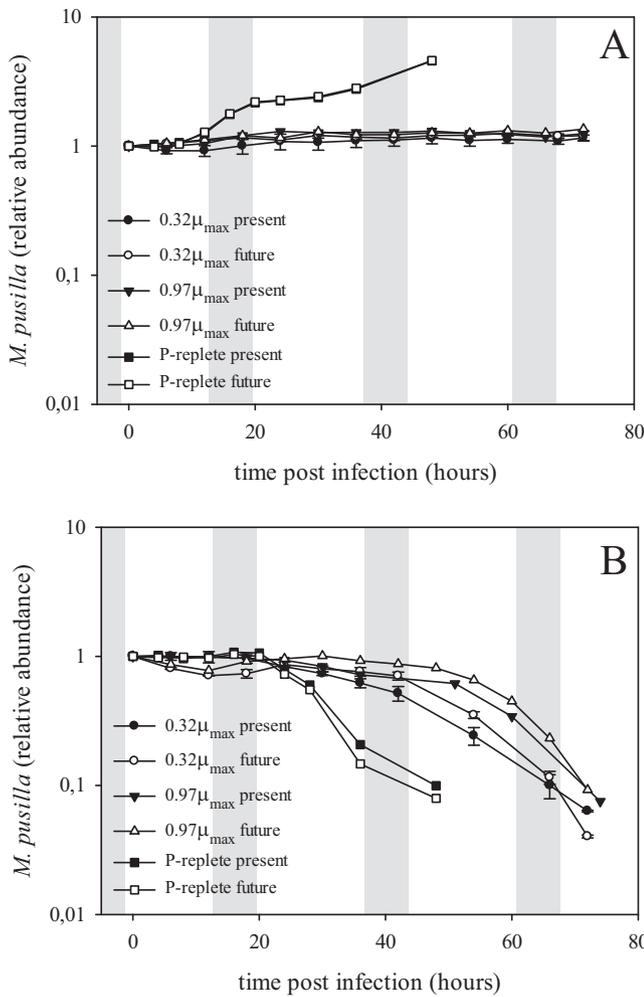
FIG 1 Algal temporal dynamics of the viral infection experiment. *Micromonas pusilla* in noninfected cultures (A) and in virally infected cultures (B). Filled symbols represent present-day (370 μatm) pCO_2, and open symbols represent future (750 μatm) pCO_2. Circles represent 0.32-μ_{max} P-limited cultures, triangles 0.97-μ_{max} P-limited cultures, and squares P-replete cultures. Abundances are normalized to the start of the experiment (T0). Gray bars represent the dark period (night). Note that the noninfected P-replete present and future pCO_2 treatments (A) fall on top of each other. Note the log scale on the *y* axis. The 0.32-μ_{max} cultures are averages from duplicate cultures.

FIG 2 Net primary production (NPP) at 4, 28, and 52 h postinfection for the noninfected controls (A) and infected cultures (B). The legend shows the different colors for 0.32-μ_{max} and 0.97-μ_{max} P-limited as well as present-day (370 μatm) and future (750 μatm) treatments. T is the median time of a 3-h incubation period. The error bars are of triplicate NPP incubations.

creased abundances of *M. pusilla* under high pCO_2 and P-limiting conditions in our study were accompanied by higher ratios of cellular C:N and C:P. A similar decoupling of the uptake of C, N, and P under P limitation has been described by several authors (52–54), where the enhanced cellular C:N and C:P ratios were a combination of increased POC and decreased PON and POP. Under P-limiting conditions, the demand for *M. pusilla* for both P and N seems to decline under high pCO_2, leading to increased abundances and cellular C:N and C:P ratios. In earlier studies, these kinds of changes in N and P demand relating to pCO_2 were suggested to be the result of a reduced necessity of elements involved in carbon fixation (53). Under future pCO_2 conditions, less N would be needed for proteins such as RuBisCO and carbonic anhydrase. The demand for P would lower because of reduced rRNA or phospholipids or a lower energy demand for the functioning of carbon-concentrating mechanisms (CCMs) (48, 53,

54). Intact polar lipid (IPL) analysis did not show a change in IPL composition between the pCO_2 treatments in our study (data not shown). Typically, small-sized phytoplankton species (e.g., *M. pusilla*) are considered less likely to be limited by CO_2 due to their relatively high surface-to-volume ratio and small boundary layer (24, 55). However, a study on *M. pusilla* strain PCC-NO27 showed activation of a CCM under low pCO_2 (<100 μatm) (56). It might be that *M. pusilla* needs this mechanism only with these very low pCO_2 values to maintain maximum growth but still invests in other mechanisms to increase the rate of carbon fixation at intermediate levels of pCO_2, i.e., higher protein and rRNA contents (54). Future ocean pCO_2 would then reduce the necessity for those components and lead to higher cellular C:N and C:P ratios.

Regarding the elemental stoichiometry between the different degrees of P limitation, the most striking effect is the lower POC content for the 0.97-μ_{max} treatment than for both the 0.32-μ_{max} and the P-replete treatments. While it is coherent that the 0.97-μ_{max} P-limited culture had a lower capacity to fix inorganic carbon than the P-replete treatment, it seems counterintuitive that the 0.32-μ_{max} culture contains an amount of cellular POC similar to that of the P-replete one. However, the NPP of the 0.32-μ_{max} cultures was half that of the 0.97-μ_{max} ones, while the growth of these cells was only 30% of that of the 0.97-μ_{max} cultures. Thus,
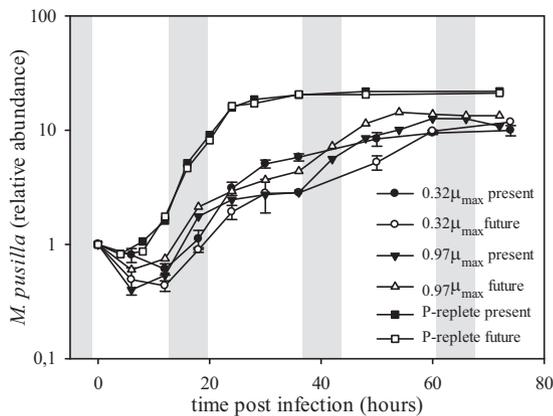
FIG 3 Temporal dynamics of *Micromonas pusilla* virus (MpV). Filled symbols represent present-day (370 μatm) pCO_2, and open symbols represent future (750 μatm) pCO_2. Circles represent 0.32-μ_{max} P-limited (0.32) algal cultures, triangles represent 0.97-μ_{max} P-limited (0.97) cultures, and squares represent P-replete cultures (P-rep). Abundances are normalized to the start of the experiment (T0). Gray bars represent the dark period (night). Note the log scale on the *y* axis. The 0.32-μ_{max} cultures are averages from duplicate cultures.

these cells had relatively high NPP compared to the growth rate. Carbon fixation has been proposed to be a way to deal with excess energy (57). The drastic decrease in Fv/Fm, epoxidation state, and Chl *a*/Chl *b* ratio for the 0.32-μ_{max} culture compared to the 0.97-μ_{max} and the P-replete cultures is in agreement with the necessity to dissipate excess energy for the cells under this treatment. The negative relationship between the Fv/Fm ratio and the degree of P limitation was mainly caused by an increase in cellular F0, as standardized to Chl *a*, which implies damage or inactivation of photosystem II (58). The higher RFL, independent of Chl *a* content, for the 0.32-μ_{max} treatment confirms this. In contrast, the relatively high RFL under P-replete conditions can be explained by the higher cellular Chl *a* content.

Our findings imply that *M. pusilla* will be competitively successful in the future ocean, due not only to its ability to cope with decreased pH and low phosphorus but probably also to the reduced necessity for components involved in CO_2 fixation, i.e., a lower P and N demand under elevated pCO_2. The increase of picoeukaryotes in several high-pCO_2 mesocosm experiments, including one with an increase in *Micromonas*-like phylotypes (7, 8), might be the result of these processes. The fact that the changes in *M. pusilla* elemental stoichiometry were observed only under P limitation implies that different global climate change-related processes can intensify the ecological or biogeochemical outcome of this pattern. These effects of increasing pCO_2 will be particularly likely due to an earlier onset and increased strengthening of vertical stratification due to global climate change (26, 59) and will largely depend on spatial and temporal variation in the degree of P limitation. A changing elemental stoichiometry in phytoplankton has been suggested to affect food quality for higher trophic levels and the efficiency of the biological pump (3). However, these processes would additionally depend on the relative contribution of grazing versus viral lysis to phytoplankton mortality.

Interaction with MpV. Elevated pCO_2 under P-limiting growth conditions resulted in increased C:P ratios of *M. pusilla*; however, this did not affect the virus growth cycle upon viral infection of *M. pusilla*. To our knowledge, there are only a few other

studies on the effects of ocean acidification on virus-phytoplankton interactions. The eclipse period of cyanophage S-PM2 infecting *Synechococcus* sp. strain WH7803 increased, and the burst size decreased with decreasing pH (8, 7.6, and 7); however, this was most likely the result of reduced host growth rate with decreasing pH (60, 61). Another laboratory study showed that the initial growth rate of *P. pouchetii* was slightly reduced by elevated pCO_2 (700 versus 350 μatm) without affecting the burst size of *P. pouchetii* virus (PpV01) (62). The same authors found a 3-fold higher burst size of *E. huxleyi* virus (EhV-99B1) infecting *E. huxleyi* strain BOF under high-pCO_2 conditions compared to the level at present-day pCO_2; however, a similar increment in burst size was observed for the preindustrial CO_2 level of 280 μatm. In contrast, a mesocosm study reported slightly reduced abundances of EhV at higher CO_2 levels without significant variation in *E. huxleyi* host abundance with pCO_2 (700 and 1,050 versus 350 μatm) (63). At the same time, the abundance of an unidentified high-fluorescence virus cluster (detected by flow cytometry) decreased up to 2-fold with increasing pCO_2, while other virus clusters were unaffected by the CO_2 level. The data on this topic are still scarce and ambiguous, and more study is needed to allow for general conclusions on the impact of viruses on marine microbes, a topic of great importance in models of climate change research (64).

In contrast to pCO_2, our study shows that P limitation strongly affected the virus growth characteristics. The latent period correlated with the level of P limitation (0.32, 0.97, and 1.0 μ_{max}), and the burst size decreased by 80% under P-limiting conditions. P depletion has also been shown to halve the burst size of PpV in *P. pouchetti* (19) and reduce the burst size of *Paramecium bursaria Chlorella* virus in *Chlorella* sp. by 90% (22). Furthermore, P-depleted blooms of *E. huxleyi* in mesocosms showed lower EhV production, most likely due to reduced burst sizes (18). Wilson and coworkers (20) studied the effect of P limitation on the interaction between *Synechococcus* sp. strain WH7803 and its phage S-PM2. A reduced production of phage under P starvation was attributed to induced pseudolysogeny rather than reduced burst size. In a P-limited mesocosm study it was later shown that P addition indeed induced the lytic cycle, resulting in increased cyanophage abundances and a collapse of the *Synechococcus* sp. bloom (65).

Although P stress has been shown to negatively affect virus production, to our knowledge this is the first report on a prolonged latent period for an algal virus. Moreover, most studies have focused on P depletion, while only under well-controlled P limitation (e.g., obtained by chemostat cultures at specific growth rates) can all host cells be maintained under the same physiological conditions. The degree of P limitation substantially prolonged the latent period, from 4 to 8 h for the P-replete cultures to 6 to 12 h for the 0.97-μ_{max} P-limited cultures and 12 to 18 h for the 0.32-μ_{max} ones. It has been proposed that viral replication is particularly sensitive to P limitation due to the relatively low C:P ratio of viruses (18). Brown and colleagues (66) showed an apparent utilization of the host genome by MpV for DNA synthesis, strengthening the idea that viral replication is indeed rate limited by substrate. However, MpV replication has been found to halt in the dark (21, 66). Considering the importance of P in photophosphorylation and as an obligatory component in intracellular energy transfer and storage, MpV replication under P limitation might also be caused by reduced energy availability. The impairment of *M. pusilla* photophysiology under P limitation and the concurrent

inhibiting effects on viral replication reported in the present study reinforce this hypothesis.

In our study, we have created a range of conditions simulating natural spatial (e.g., from coast to open ocean) and temporal (e.g., from spring to summer or from mixed to vertically stratified) gradients of P availability (23, 67). With a P-replete area or season as a point of reference, first a prolongation of the latent period and then a decrease in burst size will be encountered when moving to more P-limited conditions. The latent period is further prolonged at the point in space or time where P limitation affects the growth rate of the algal host. As global warming of the surface ocean (e.g., the north Atlantic Ocean [68]) is expected to lead to increased vertical stratification (25), P limitation will be enhanced due to reduced nutrient supply from deeper waters (possibly strengthened due to enhanced diazotroph N input [69]). Thus, viral infection of *M. pusilla* in the future ocean is likely to be inhibited. Theoretically a lower impact of viruses leads to a less regenerative system. However, to what extent the presence of organic phosphorus compounds, which can be up to 5 times as high as the soluble reactive (inorganic) phosphorus concentration in the open ocean (70), can counteract this effect is still unknown. Certain phytoplankton groups have been shown to be able to utilize different compounds, such as phosphomonoesters and nucleotides (71). The presence of alkaline phosphatase in *M. pusilla* suggests that it is able to assimilate certain organic phosphorus compounds. P limitation of picophotoautotrophs in the oligotrophic ocean then could be relieved, overcoming the negative effects of host P limitation on virus production. The capability of an infected algal host cell to assimilate P during viral proliferation remains to be studied, but it can be expected to have a similar countering result. In a future P-limited ocean, the elevated pCO_2 will lead to increased cell abundance of *M. pusilla*, thereby enhancing the virus-host contact rate and possibly compensating for the prolonged latent period due to increased P limitation. Thus, the final outcome for the picoeukaryote host population, food web efficiency, and carbon export to deeper waters would depend on the original degree of P stress (trophic state). The current study advances our limited understanding of the influence of enhanced pCO_2 and P stress on virally infected picoeukaryote photoautotrophs while at the same time stressing the importance of additional research, including that on other ecologically relevant phytoplankton species and ecotypes.

Conclusions. To date, many laboratory studies have focused on the ability of phytoplankton to cope with increasing pCO_2 conditions, but typically the focus has been on the larger size classes. This study showed a beneficial effect of elevated pCO_2 on the cell abundance and cellular C:N and C:P ratios of the picoeukaryote *M. pusilla* under P limitation, which confirms earlier findings of stimulated growth of picoeukaryotes under future CO_2 levels (7–9). However, the effects on cell stoichiometry will play a role only under nutrient (i.e., P)-limiting conditions. Moreover, we showed that viral lysis is an important aspect to consider when studying the impact of global climate change on ecosystem functioning. Although virus-host interactions were not directly affected by pCO_2, growth under P limitation led to longer latent periods and strongly reduced viral burst sizes. These results suggest that when P limitation prevails in future oceans, picoeukaryotes and grazing will be favored over larger-sized phytoplankton and viral lysis with increased matter and nutrient flow to higher trophic levels. Our current results suggest that in a stratified future ocean, viral lysis will have a decreased impact on phytoplankton mortality with possible subsequent negative feedback on the cycling of carbon and nutrients in the water column. However, to what extent uptake of organic P and P utilization during infection will adjust the ecological and biogeochemical impact needs further study.

ACKNOWLEDGMENTS

REFERENCES

1. **Meehl GA, Stocker TF, Collins WD, Friedlingstein P, Gaye AT, Gregory JM, Kitoh A, Knutti R, Murphy JM, Noda A, Raper SCB, Watterson IG, Weaver AJ, Zhao ZC.** 2007. Global climate projections, p 749–844. *In* Solomon S, Qin D, Manning M, Chen Z, Marquis M, Averyt KB, Tignor M, Miller HL (ed), Climate change 2007: the physical science basis. Contribution of Working Group I to the Fourth Assessment Report of the Intergovernmental Panel on Climate Change. Cambridge University Press, Cambridge, United Kingdom.

2. **Sabine CL, Feely RA, Gruber N, Key RM, Lee K, Bullister JL, Wanninkhof R, Wong CS, Wallace DWR, Tilbrook B, Millero FJ, Peng TH, Kozyr A, Ono T, Rios AF.** 2004. The oceanic sink for anthropogenic CO_2. Science **305:**367–371. http://dx.doi.org/10.1126/science.1097403.

3. **Riebesell U, Tortell PD.** 2011. Effects of ocean acidification on pelagic organisms and ecosystems, p 99–121. *In* Gattuso JP, Hansson L (ed), Ocean acidification. Oxford University Press, Oxford, United Kingdom.

4. **Schaum E, Rost B, Millar AJ, Collins S.** 2012. Variation in plastic responses of a globally distributed picoplankton species to ocean acidification. Nat. Climate Change **3:**298–302. http://dx.doi.org/10.1038/nclimate1774.

5. **Giordano M, Beardall J, Raven JA.** 2005. CO_2 concentrating mechanisms in algae: mechanisms, environmental modulation, and evolution. Annu. Rev. Plant Biol. **56:**99–131. http://dx.doi.org/10.1146/annurev.arplant.56.032604.144052.

6. **Worden AZ, Lee J-H, Mock T, Rouze P, Simmons MP, Aerts AL, Allen AE, Cuvelier ML, Derelle E, Everett MV, Foulon E, Grimwood J, Gundlach H, Henrissat B, Napoli C, McDonald SM, Parker MS, Rombauts S, Salamov A, Von Dassow P, Badger JH, Coutinho PM, Demir E, Dubchak I, Gentemann C, Eikrem W, Gready JE, John U, Lanier W, Lindquist EA, Lucas S, Mayer KFX, Moreau H, Not F, Otillar R, Panaud O, Pangilinan J, Paulsen I, Piegu B, Poliakov A, Robbens S, Schmutz J, Toulza E, Wyss T, Zelensky A, Zhou K, Armbrust EV, Bhattacharya D, Goodenough UW, Van de Peer Y, Grigoriev IV.** 2009. Green evolution and dynamic adaptations revealed by genomes of the marine picoeukaryotes *Micromonas*. Science **324:**268–272. http://dx.doi.org/10.1126/science.1167222.

7. **Brussaard CPD, Noordeloos AAM, Witte H, Collenteur MCJ, Schulz K, Ludwig A, Riebesell U.** 2013. Arctic microbial community dynamics influenced by elevated CO_2 levels. Biogeosciences **10:**719–731. http://dx.doi.org/10.5194/bg-10-719-2013.

8. **Engel A, Schulz KG, Riebesell U, Bellerby R, Delille B, Schartau M.** 2008. Effects of CO_2 on particle size distribution and phytoplankton abundance during a mesocosm bloom experiment (PeECE II). Biogeosciences **5:**509–521. http://dx.doi.org/10.5194/bg-5-509-2008.

9. **Meakin NG, Wyman M.** 2011. Rapid shifts in picoeukaryote community structure in response to ocean acidification. ISME J. **5:**1397–1405. http://dx.doi.org/10.1038/ismej.2011.18.

10. **Not F, Latasa M, Marie D, Cariou T, Vaulot D, Simon N.** 2004. A single species, *Micromonas pusilla* (Prasinophyceae), dominates the eukaryotic

picoplankton in the western English channel. Appl. Environ. Microbiol. **70:**4064–4072. http://dx.doi.org/10.1128/AEM.70.7.4064-4072.2004.

11. **Slapeta J, Lopez-Garcia P, Moreira D.** 2006. Global dispersal and ancient cryptic species in the smallest marine eukaryotes. Mol. Biol. Evol. **23:**23–29. http://dx.doi.org/10.1093/molbev/msj001.

12. **Mayer JA.** 1977. Viral infection in marine Prasinophycean alga, *Micromonas pusilla*. J. Phycol. **13:**229–301.

13. **Cottrell MT, Suttle CA.** 1995. Dynamics of a lytic virus infecting the photosynthetic marine picoflagellate *Micromonas pusilla*. Limnol. Oceanogr. **40:**730–739. http://dx.doi.org/10.4319/lo.1995.40.4.0730.

14. **Wilhelm SW, Suttle CA.** 1999. Viruses and nutrient cycles in the sea–viruses play critical roles in the structure and function of aquatic food webs. Bioscience **49:**781–788. http://dx.doi.org/10.2307/1313569.

15. **Brussaard CPD, Wilhelm SW, Thingstad F, Weinbauer MG, Bratbak G, Heldal M, Kimmance SA, Middelboe M, Nagasaki K, Paul JH, Schroeder DC, Suttle CA, Vaque D, Wommack KE.** 2008. Global-scale processes with a nanoscale drive: the role of marine viruses. ISME J. **2:**575–578. http://dx.doi.org/10.1038/ismej.2008.31.

16. **Hennes KP, Suttle CA, Chan AM.** 1995. Fluorescently labeled virus probes show that natural virus populations can control the structure of marine microbial communities. Appl. Environ. Microbiol. **61:**3623–3627.

17. **Suttle CA.** 2007. Marine viruses—major players in the global ecosystem. Nat. Rev. Microbiol. **5:**801–812. http://dx.doi.org/10.1038/nrmicro1750.

18. **Bratbak G, Egge JK, Heldal M.** 1993. Viral mortality of the marine alga *Emiliania huxleyi* (Haptophyceae) and termination of algal blooms. Mar. Ecol. Prog. Ser. **93:**39–48. http://dx.doi.org/10.3354/meps093039.

19. **Bratbak G, Jacobsen A, Heldal M, Nagasaki K, Thingstad F.** 1998. Virus production in *Phaeocystis pouchetii* and its relation to host cell growth and nutrition. Aquat. Microb. Ecol. **16:**1–9. http://dx.doi.org/10.3354/ame016001.

20. **Wilson WH, Carr NG, Mann NH.** 1996. The effect of phosphate status on the kinetics of cyanophage infection in the oceanic cyanobacterium *Synechococcus* sp. WH7803. J. Phycol. **32:**506–516. http://dx.doi.org/10.1111/j.0022-3646.1996.00506.x.

21. **Baudoux A-C, Brussaard CPD.** 2008. Influence of irradiance on virus-algal host interactions. J. Phycol. **44:**902–908. http://dx.doi.org/10.1111/j.1529-8817.2008.00543.x.

22. **Clasen JL, Elser JJ.** 2007. The effect of host *Chlorella* NC64A carbon:phosphorus ratio on the production of *Paramecium bursaria Chlorella* virus-1. Freshw. Biol. **52:**112–122. http://dx.doi.org/10.1111/j.1365-2427.2006.01677.x.

23. **Dyhrman ST, Ammerman JW, Van Mooy BAS.** 2007. Microbes and the marine phosphorus cycle. Oceanography **20:**110–116. http://dx.doi.org/10.5670/oceanog.2007.54.

24. **Raven JA.** 1998. The twelfth Tansley lecture. Small is beautiful: the picophytoplankton. Funct. Ecol. **12:**503–513.

25. **Sarmiento JL, Slater R, Barber R, Bopp L, Doney SC, Hirst AC, Kleypas J, Matear R, Mikolajewicz U, Monfray P, Soldatov V, Spall SA, Stouffer R.** 2004. Response of ocean ecosystems to climate warming. Glob. Biogeochem. Cycles **18:**1–23. http://dx.doi.org/10.1029/2003GB002134.

26. **Behrenfeld MJ, O'Malley RT, Siegel DA, McClain CR, Sarmiento JL, Feldman GC, Milligan AJ, Falkowski PG, Letelier RM, Boss ES.** 2006. Climate-driven trends in contemporary ocean productivity. Nature **444:**752–755. http://dx.doi.org/10.1038/nature05317.

27. **Suttle CA.** 1993. Enumeration and isolation of viruses, p 121–134. *In* Kemp PF, Sherr BF, Sherr EF, Cole JJ (ed), Current methods in aquatic microbial ecology. Lewis Publishers, Boca Raton, FL.

28. **Guillard RR, Ryther JH.** 1962. Studies of marine planktonic diatoms. 1. *Cylotella nana hustedt* and *Detonula convervacea* (cleve) *gran*. Can. J. Microbiol. **8:**229–239.

29. **Cottrell MT, Suttle CA.** 1991. Wide-spread occurrence and clonal variation in viruses which cause lysis of a cosmopolitan, eukaryotic marine phytoplankter, *Micromonas pusilla*. Mar. Ecol. Prog. Ser. **78:**1–9. http://dx.doi.org/10.3354/meps078001.

30. **Schulz KG, Barcelos e Ramos J, Zeebe RE, Riebesell U.** 2009. CO_2 perturbation experiments: similarities and differences between dissolved inorganic carbon and total alkalinity manipulations. Biogeosciences **6:**2145–2153. http://dx.doi.org/10.5194/bg-6-2145-2009.

31. **Hoogstraten A, Peters M, Timmermans KR, de Baar HJW.** 2012. Combined effects of inorganic carbon and light on *Phaeocystis globosa* Scherffel (Prymnesiophyceae). Biogeosciences **9:**1885–1896. http://dx.doi.org/10.5194/bg-9-1885-2012.

32. **Marie D, Brussaard CPD, Thyrhaug R, Bratbak G, Vaulot D.** 1999. Enumeration of marine viruses in culture and natural samples by flow cytometry. Appl. Environ. Microbiol. **65:**45–52.

33. **Brussaard CPD.** 2004. Optimization of procedures for counting viruses by flow cytometry. Appl. Environ. Microbiol. **70:**1506–1513. http://dx.doi.org/10.1128/AEM.70.3.1506-1513.2004.

34. **Vaulot D.** 1989. CYTOPC: processing software for flow cytometric data. Signal Noise **2:**8.

35. **Dickson AG, Goyet C (ed).** 1994. Handbook of methods for the analysis of the various parameters of the carbon dioxide system in sea water, version 2. ORNL/CDIAC-74. Carbon Dioxide Information Analysis Center, Oak Ridge National Laboratory, Oak Ridge, TN.

36. **Dickson AG, Sabine CL, Christian JR (ed).** 2007. Guide to the best practices for ocean CO_2 measurements. PICES special publication 3. Carbon Dioxide Information Analysis Center, Oak Ridge National Laboratory, Oak Ridge, TN.

37. **Lewis E, Wallace DWR.** 1998. Program developed for CO_2 system calculations. Carbon Dioxide Information Analysis Center, Oak Ridge National Laboratory, Oak Ridge, TN.

38. **Mehrbach C, Culberso CH, Hawley JE, Pytkowic RM.** 1973. Measurement of apparent dissociation constants of carbonic acid in seawater at atmospheric pressure. Limnol. Oceanogr. **18:**897–907. http://dx.doi.org/10.4319/lo.1973.18.6.0897.

39. **Dickson AG, Millero FJ.** 1987. A comparison of the equilibrium constants for the dissociation of carbonic acid in seawater media. Deep Sea Res. A Oceanogr. Res. Pap. **34:**1733–1743. http://dx.doi.org/10.1016/0198-0149(87)90021-5.

40. **Takahashi T, Sutherland SC, Sweeney C, Poisson A, Metzl N, Tilbrook B, Bates N, Wanninkhof R, Feely RA, Sabine C, Olafsson J, Nojiri Y.** 2002. Global sea-air CO_2 flux based on climatological surface ocean pCO_2, and seasonal biological and temperature effects. Deep Sea Res. Part 2 Top. Stud. Oceanogr. **49:**1601–1622. http://dx.doi.org/10.1016/S0967-0645(02)00003-6.

41. **Hansen HP, Koroleff F.** 1999. Determination of nutrients, p 125–187. *In* Grasshoff K, Kremling K, Erhardt M (ed), Methods of seawater analysis, 3rd ed. Wiley, Weinheim, Germany.

42. **Perry MJ.** 1972. Alkaline phosphatase activity in subtropical central north pacific waters using a sensitive fluorometric method. Mar. Biol. **15:**113–115. http://dx.doi.org/10.1007/BF00353639.

43. **Verardo DJ, Froelich PN, McIntyre A.** 1990. Determination of organic-carbon and nitrogen in marine-sediments using the Carlo-Erba-NA-1500 analyzer. Deep Sea Res. A Oceanogr. Res. Pap. **37:**157–165. http://dx.doi.org/10.1016/0198-0149(90)90034-S.

44. **Genty B, Briantais JM, Baker NR.** 1989. The relationship between the quantum yield of photosynthetic electron transport and quenching of chlorophyll fluorescence. Biochim. Biophys. Acta **990:**87–92. http://dx.doi.org/10.1016/S0304-4165(89)80016-9.

45. **Steeman-Nielsen E.** 1952. The use of radioactive carbon (^{14}C) for measuring organic production in the sea. J. Cons. Int. Explor. Mer **18:**117–140. http://dx.doi.org/10.1093/icesjms/18.2.117.

46. **Zapata M, Rodriguez F, Garrido JL.** 2000. Separation of chlorophylls and carotenoids from marine phytoplankton: a new HPLC method using a reversed phase C_8 column and pyridine-containing mobile phases. Mar. Ecol. Prog. Ser. **195:**29–45. http://dx.doi.org/10.3354/meps195029.

47. **Geider RJ, Laroche J, Greene RM, Olaizola M.** 1993. Response of the photosynthetic apparatus of *Phaeodactylum tricornutum* (Bacillariophyceae) to nitrate, phosphate, or iron starvation. J. Phycol. **29:**755–766. http://dx.doi.org/10.1111/j.0022-3646.1993.00755.x.

48. **Borchard C, Borges AV, Haendel N, Engel A.** 2011. Biogeochemical response of *Emiliania huxleyi* (PML B92/11) to elevated CO_2 and temperature under phosphorous limitation: a chemostat study. J. Exp. Mar. Biol. Ecol. **410:**61–71. http://dx.doi.org/10.1016/j.jembe.2011.10.004.

49. **McCarthy A, Rogers SP, Duffy SJ, Campbell DA.** 2012. Elevated carbon dioxide differentially alters the photophysiology of *Thalassiosira pseudonana* (Bacillariophyceae) and *Emiliania huxleyi* (Haptophyta). J. Phycol. **48:**635–646. http://dx.doi.org/10.1111/j.1529-8817.2012.01171.x.

50. **Schulz KG, Bellerby R, Brussaard C, Büdenbender J, Czerny J, Engel A, Fischer M, Koch-Klavsen S, Krug S, Lischka S.** 2012. Temporal biomass dynamics of an Arctic plankton bloom in response to increasing levels of atmospheric carbon dioxide. Biogeosci. Discuss. **9:**12543–12592. http://dx.doi.org/10.5194/bgd-9-12543-2012.

51. **DuRand MD, Green RE, Sosik HM, Olson RJ.** 2002. Diel variations in optical properties of *Micromonas pusilla* (Prasinophyceae). J. Phycol. **38:**1132–1142. http://dx.doi.org/10.1046/j.1529-8817.2002.02008.x.

52. **Sakshaug E, Holmhansen O.** 1977. Chemical composition of *Skeletonema costatum* (Grev.) Cleve and *Pavlova* (*monochrysis*) *lutheri* (droop) green as a function of nitrate-, phosphate-, and iron-limited growth. J. Exp. Mar. Biol. Ecol. **29:**1–34. http://dx.doi.org/10.1016/0022-0981(77)90118-6.

53. **Beardall J, Johnston A, Raven J.** 1998. Environmental regulation of CO_2-concentrating mechanisms in microalgae. Can. J. Bot. **76:**1010–1017. http://dx.doi.org/10.1139/b98-079.

54. **Reinfelder JR.** 2012. Carbon dioxide regulation of nitrogen and phosphorus in four species of marine phytoplankton. Mar. Ecol. Prog. Ser. **466:**57–67. http://dx.doi.org/10.3354/meps09905.

55. **Finkel ZV, Beardall J, Flynn KJ, Quigg A, Rees TAV, Raven JA.** 2010. Phytoplankton in a changing world: cell size and elemental stoichiometry. J. Plankton Res. **32:**119–137. http://dx.doi.org/10.1093/plankt/fbp098.

56. **Iglesias-Rodriguez MD, Nimer NA, Merrett MJ.** 1998. Carbon dioxide-concentrating mechanism and the development of extracellular carbonic anhydrase in the marine picoeukaryote *Micromonas pusilla*. New Phytol. **140:**685–690. http://dx.doi.org/10.1046/j.1469-8137.1998.00309.x.

57. **Norici A, Bazzoni AM, Pugnetti A, Raven JA, Giordano M.** 2011. Impact of irradiance on the C allocation in the coastal marine diatom *Skeletonema marinoi* Sarno and Zingone. Plant Cell Environ. **34:**1666–1677. http://dx.doi.org/10.1111/j.1365-3040.2011.02362.x.

58. **Yamane Y, Kashino Y, Koike H, Satoh K.** 1997. Increases in the fluorescence F_o level and reversible inhibition of photosystem II reaction center by high-temperature treatments in higher plants. Photosynth. Res. **52:**57–64. http://dx.doi.org/10.1023/A:1005884717655.

59. **Forster P, Ramaswamy V, Artaxo P, Berntsen T, Betts R, Fahey DW, Haywood J, Lean J, Lowe DC, Myhre G, Nganga J, Prinn R, Raga G, Schulz M, van Dorland R.** 2007. Changes in atmospheric constituents and in radiative forcing. *In* Solomon S, Qin D, Manning M, Chen Z, Marquis M, Averyt KB, Tignor M, Miller HL (ed), Climate change 2007: the physical science basis. Contribution of Working Group I to the Fourth Assessment Report of the Intergovernmental Panel on Climate Change. Cambridge University Press, Cambridge, United Kingdom.

60. **Traving SJ, Clokie MRJ, Middelboe M.** 2013. Increased acidification has a profound effect on the interactions between the cyanobacterium *Synechococcus* sp. WH7803 and its viruses. FEMS Microbiol. Ecol. **87:**133–141. http://dx.doi.org/10.1111/1574-6941.12199.

61. **Middelboe M.** 2000. Bacterial growth rate and marine virus-host dynamics. Microb. Ecol. **40:**114–124.

62. **Carreira C, Heldal M, Bratbak G.** 2013. Effect of increased pCO_2 on phytoplankton-virus interactions. Biogeochemistry **114:**391–397. http://dx.doi.org/10.1007/s10533-011-9692-x.

63. **Larsen JB, Larsen A, Thyrhaug R, Bratbak G, Sandaa RA.** 2008. Response of marine viral populations to a nutrient induced phytoplankton bloom at different pCO_2 levels. Biogeosciences **5:**523–533. http://dx.doi.org/10.5194/bg-5-523-2008.

64. **Danovaro R, Corinaldesi C, Dell'Anno A, Fuhrman JA, Middelburg JJ, Noble RT, Suttle CA.** 2011. Marine viruses and global climate change. FEMS Microbiol. Rev. **35:**993–1034. http://dx.doi.org/10.1111/j.1574-6976.2010.00258.x.

65. **Wilson WH, Turner S, Mann NH.** 1998. Population dynamics of phytoplankton and viruses in a phosphate-limited mesocosm and their effect on DMSP and DMS production. Estuar. Coast. Shelf Sci. **46:**49–59. http://dx.doi.org/10.1006/ecss.1998.0333.

66. **Brown CM, Campbell DA, Lawrence JE.** 2007. Resource dynamics during infection of *Micromonas pusilla* by virus MpV-Sp1. Environ. Microbiol. **9:**2720–2727. http://dx.doi.org/10.1111/j.1462-2920.2007.01384.x.

67. **Moore C, Mills M, Arrigo K, Berman-Frank I, Bopp L, Boyd P, Galbraith E, Geider R, Guieu C, Jaccard S.** 2013. Processes and patterns of oceanic nutrient limitation. Nat. Geosci. **6:**701–710. http://dx.doi.org/10.1038/ngeo1765.

68. **Polovina JJ, Howell EA, Abecassis M.** 2008. Ocean's least productive waters are expanding. Geophys. Res. Lett. **35:**L03618. http://dx.doi.org/10.1029/2007GL031745.

69. **Karl D, Letelier R, Tupas L, Dore J, Christian J, Hebel D.** 1997. The role of nitrogen fixation in biogeochemical cycling in the subtropical North Pacific Ocean. Nature **388:**533–538. http://dx.doi.org/10.1038/41474.

70. **Karl D, Bjorkman KM.** 2002. Dynamics of DOP, p 249–366. *In* Hansell D, Carlson CA (ed), Biogeochemistry of marine dissolved matter. Academic, London, United Kingdom.

71. **Wang Z-H, Liang Y, Kang W.** 2011. Utilization of dissolved organic phosphorus by different groups of phytoplankton taxa. Harmful Algae **12:**113–118. http://dx.doi.org/10.1016/j.hal.2011.09.005.